Mon. Not. R. Astron. Soc. **356,** 1592–1598 (2005) doi:10.1111/j.1365-2966.2005.08637.x

Emission lines of Fe XV in spectra obtained with the Solar Extreme-Ultraviolet Research Telescope and Spectrograph

F. P. Keenan,[1⋆] K. M. Aggarwal,[1] R. O. Milligan,[1,2] R. S. I. Ryans,[1] D. S. Bloomfield,[1] V. Srigengan,[1] M. G. O'Mullane,[3] K. D. Lawson,[3] A. Z. Msezane,[4] J. W. Brosius,[2,5] J. M. Davila[2] and R. J. Thomas[2]

[1]*Department of Physics and Astronomy, Queen's University, Belfast BT7 1NN*
[2]*Laboratory for Astronomy and Solar Physics, Code 682, NASA's Goddard Space Flight Center, Greenbelt, MD 20771, USA*
[3]*EURATOM-UKAEA Fusion Association, Culham Science Centre, Abingdon OX14 3DB*
[4]*Center for Theoretical Studies of Physical Systems, Clark Atlanta University, Atlanta, GA 30304, USA*
[5]*Department of Physics, The Catholic University of America, Washington, DC 20064, USA*

Accepted 2004 November 11. Received 2004 November 11; in original form 2004 October 15

ABSTRACT

Recent R-matrix calculations of electron impact excitation rates in Mg-like Fe XV are used to derive theoretical emission-line ratios involving transitions in the 243–418 Å wavelength range. A comparison of these with a data set of solar active region, subflare and off-limb spectra, obtained during rocket flights by the Solar Extreme-Ultraviolet Research Telescope and Spectrograph (SERTS), reveals generally very good agreement between theory and observation, indicating that most of the Fe XV emission lines may be employed with confidence as electron density diagnostics. In particular, the 312.55-Å line of Fe XV is not significantly blended with a Co XVII transition in active region spectra, as suggested previously, although the latter does make a major contribution in the subflare observations. Most of the Fe XV transitions which are blended have had the species responsible clearly identified, although there remain a few instances where this has not been possible. We briefly address the long-standing discrepancy between theory and experiment for the intensity ratio of the $3s^2\,{}^1S$–$3s3p\,{}^3P_1$ intercombination line at 417.25 Å to the $3s^2\,{}^1S$–$3s3p\,{}^1P$ resonance transition at 284.16 Å.

Key words: atomic data – Sun: activity – Sun: flares – ultraviolet: general.

1 INTRODUCTION

Emission features arising from transitions in Mg-like Fe XV are widely detected in solar extreme-ultraviolet (EUV) spectra, with the $3s^2\,{}^1S$–$3s3p\,{}^1P$ resonance line at 284.16 Å being one of the most intense in this spectral region (see, for example, Dere 1978; Thomas & Neupert 1994). The usefulness of these lines as electron density diagnostics for the emitting plasma was first noted by Bely & Blaha (1968). Since then, many authors have produced theoretical line ratios for Fe XV applicable to solar spectra (see Kastner & Bhatia 2001, and references therein).

The most detailed comparison to date between theory and experiment for solar EUV transitions in Fe XV is probably that by Young, Landi & Thomas (1998). These authors employed the high-resolution active region spectrum obtained by the Solar EUV Rocket Telescope and Spectrograph (SERTS) during a flight in 1989, which was compared with line ratios generated from the CHIANTI data base (Dere et al. 1997). However, since the 1989 campaign there have been several further flights of SERTS (now called the Solar EUV Research Telescope and Spectrograph), which have observed a wider range of solar features, and measured additional Fe XV lines not present in the 1989 active region spectrum. Also, the 1989 flight of SERTS obtained a subflare spectrum, not analysed by Young et al. (1998).

In this paper we present new line ratio calculations for Fe XV, derived using the most recent atomic physics data. We assess the usefulness and accuracy of these diagnostics via a comparison with the extensive data sets obtained by SERTS during several sounding rocket experiments, including those of several active regions, plus a subflare and an off-limb area.

2 OBSERVATIONAL DATA

The solar spectra analysed in the present paper are those of several active regions, a small subflare, and an off-limb area, obtained with the SERTS instrument (Neupert et al. 1992) which was developed by the National Aeronautics and Space Administration (NASA) Goddard Space Flight Center. Most of these

⋆E-mail: F.Keenan@qub.ac.uk

Table 1. Fe XV transitions and line ratio designations.

Transition	λ (Å)	$R = I(\lambda)/I(327.03\ \text{Å})$
$3s3p\ ^1P–3s3d\ ^1D$	243.78	R_1
$3s^2\ ^1S–3s3p\ ^1P$	284.16	R_2
$3s3p\ ^3P_1–3p^2\ ^3P_2$	292.25	R_3
$3s3p\ ^3P_0–3p^2\ ^3P_1$	302.32	R_4
$3s3p\ ^3P_2–3p^2\ ^3P_2$	304.87	R_{11}
$3s3p\ ^3P_1–3p^2\ ^3P_1$	307.76	R_{12}
$3s3p\ ^3P_1–3p^2\ ^1D$	312.55	R_{14}
$3s3p\ ^3P_1–3p^2\ ^3P_0$	317.64	R_5
$3s3p\ ^3P_2–3p^2\ ^3P_1$	321.78	R_{13}
$3s3p\ ^1P–3p^2\ ^1S$	324.97	R_6
$3s3p\ ^3P_2–3p^2\ ^1D$	327.03	–
$3s3d\ ^3D_3–3p3d\ ^3P_2$	330.99	R_7
$3s3d\ ^3D_3–3p3d\ ^3F_4$	372.76	R_8
$3s^2\ ^1S–3s3p^3P_2$	393.97	R_9
$3s^2\ ^1S–3s3p^3P_1$	417.25	R_{10}

observations span the 232–445 Å wavelength range in first order, and were recorded on Eastman Kodak 101–07 emulsion during SERTS rocket flights on 1989 May 5 (SERTS–89), 1991 May 7 (SERTS–91) and 1993 August 17 (SERTS–93). The flight on 1997 November 18 (SERTS–97) used an intensified CCD camera covering the 299–353 Å bandpass, which detected several Fe XV emission lines not recorded on previous missions, such as 302.32 and 324.97 Å. In addition, SERTS–97 was exceptionally well calibrated, so that its measured intensity ratios should be the most reliable. Several quiet regions were also observed during the SERTS flights, but the intensities of the Fe XV emission lines were too low to permit a reliable analysis. We note that the SERTS flight on 1995 May 15 had a multilayer-coated grating that enhanced the second-order response while suppressing first-order, making the intensity calibration very uncertain for wavelengths greater than 340 Å (Brosius, Davila & Thomas 1998).

The spectral resolutions of the SERTS data recorded on film are typically 50–80 mÅ (FWHM), while those of the SERTS–97 observations are 115 mÅ. Intrinsic spatial resolutions in all cases are approximately 7 arcsec (FWHM), although the analysed spectra were averaged over spatial scales appropriate for the solar feature being observed in order to improve measurement precision. Further details of the observations, and the wavelength and absolute flux calibration procedures employed in the data reduction, may be found in Thomas & Neupert (1994) for the SERTS–89 spectra, in Brosius et al. (1996) for SERTS–91 and SERTS–93, and in Brosius et al. (2000) for SERTS–97.

In Table 1 we list the Fe XV emission lines measured in the SERTS spectral range by Thomas & Neupert (1994) and Brosius et al. (2000), as well as the identification of the 393.97-Å transition suggested by Brickhouse, Raymond & Smith (1995). The $3s3p^3\ P_1–3p^2\ ^3P_2$ transition of Fe XV was originally identified as the emission line at 292.39 Å in the SERTS–89 active region spectrum by Thomas & Neupert. However, Young et al. (1998) pointed out that the Fe XV transition is actually the feature at 292.25 Å, misclassified as being due to Si X, as also noted by Keenan et al. (2000).

A search of line lists, such as the Atomic Line List of Peter van Hoof (http://star.pst.qub.ac.uk/∼pvh) suggests possible identifications for the 292.39-Å feature of the $3s^23p^3\ ^2D_{5/2}–3s3p^4\ ^2D_{5/2}$ transition of Ni XIV and/or the Ne VIII $1s^23d\ ^2D_{3/2}–1s^2\ 4f^2F_{7/2}$ line. Calculations with the latest version (4.2) of the CHIANTI data base (Dere et al. 1997; Young et al. 2003) for the isoelectronic Fe XII ion (as Ni XIV is not in CHIANTI) indicate that the Ni XIV $3s^23p^3\ ^2D_{5/2}–3s3p^4\ ^2D_{5/2}$ line should be of similar intensity to the $3s^23p^3\ ^4S–3s3p^4\ ^4P_{5/2}$ feature at 316.60 Å. However, in the SERTS–89 active region spectrum the 292.39-Å feature is about a factor of 5.6 stronger than that at 316.60 Å, ruling out Ni XIV as a possible identification. Similarly, we have used CHIANTI to generate a synthetic active region spectrum, which indicates that the Ne VIII transition should be about 2 per cent of the intensity of the nearby Si IX 292.80-Å line. In fact, the 292.39- and 292.80-Å features are observed to be comparable in strength, ruling out Ne VIII as a likely blending candidate. We have also checked for possible second-order lines (i.e. features around 146.20 Å) which might blend in with first-order transitions, but no strong features are predicted by CHIANTI. Thus, it is not clear what the source of the 292.39-Å feature is, and its identification clearly requires further work.

Intensities of the Fe XV emission lines listed in Table 1 were determined by using the spectrum synthesis package DIPSO (Howarth, Murray & Mills 1994) to fit Gaussian profiles to the SERTS observations. The results for the 327.03-Å feature are listed in the notes to Tables 2–5; observed intensities of the other Fe XV transitions may be inferred from these using the line ratios given in the tables (see Section 3). Also given in the table notes are the first-order bandpasses of the SERTS data sets.

Observational uncertainties in the line intensities have been determined using methods discussed in detail by Thomas & Neupert (1994). The intensities and uncertainties quoted here are different from those originally reported in the papers referenced above, because the spectral data have been completely reanalysed by a standard fitting procedure to ensure consistency of the results. Also, a uniform factor of 1.24 has been applied here to all SERTS–89 intensities, reflecting a more recent re-evaluation of its absolute calibration scale. Even so, in all directly comparable cases, the resulting intensity ratios differ only slightly from those obtained using previously published data.

The quality of the Fe XV observational data are illustrated in Figs 1–4, where we plot several portions of the SERTS spectra for a variety of solar features measured on different flights of the rocket payload. We note that each SERTS spectrum exhibits a background level due to film fog, scattered light and actual solar continuum. The background was calculated using methods detailed in Thomas & Neupert (1994) and Brosius et al. (1996, 2000), and then subtracted

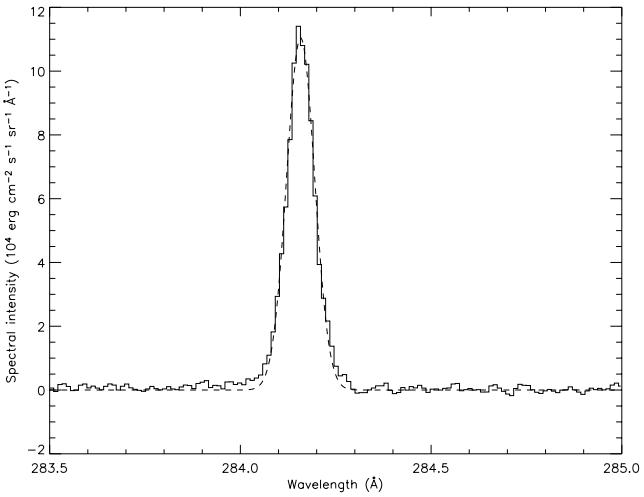

Figure 1. Plot of the SERTS–89 subflare spectrum in the 283.5–285.0 Å wavelength range. The profile fit to the Fe XV 284.16-Å feature is shown by a dashed line.

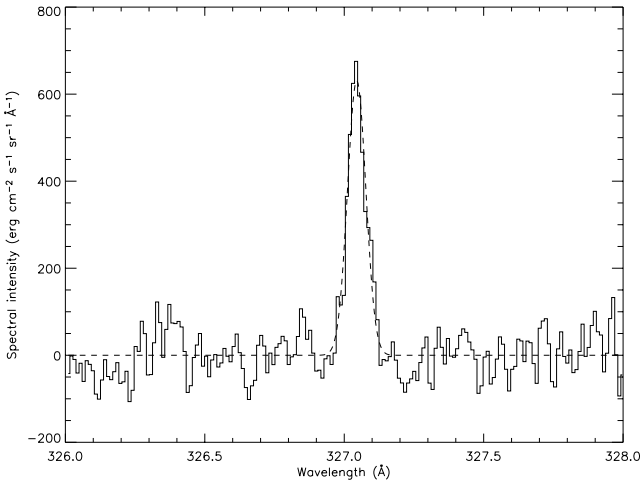

Figure 2. Plot of the SERTS–93 active region spectrum in the 326.0–328.0 Å wavelength range. The profile fit to the Fe XV 327.03-Å feature is shown by a dashed line.

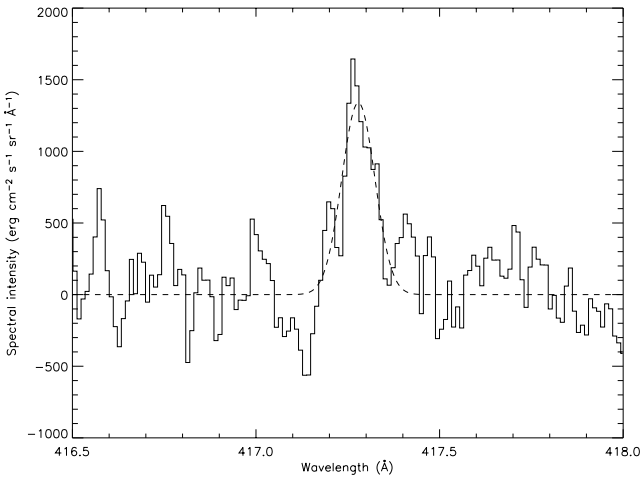

Figure 3. Plot of the SERTS–91 off-limb spectrum in the 416.5–418.0 Å wavelength range. The profile fit to the Fe XV 417.25-Å feature is shown by a dashed line.

from the initial spectrum, leaving only an emission-line spectrum (with noise) on a zero base level. It is this zero base level which is shown in Figs 1–4.

3 ADOPTED ATOMIC DATA AND THEORETICAL LINE RATIOS

The model ion for Fe XV consisted of the energetically lowest 53 fine-structure levels belonging to the $3s^2$, 3s3p, $3p^2$, 3s3d, 3p3d, $3d^2$, 3s4s, 3s4p, 3s4d, 3p4s and 3s4f configurations. Energies of these levels were obtained from Churilov et al. (1985), Churilov, Levashov & Wyart (1989), Litzen & Redfors (1987), Sugar & Corliss (1985) and Aggarwal, Keenan & Msezane (2003).

Electron impact excitation rates for transitions among the levels discussed above were taken from Aggarwal et al. (2003). For Einstein A coefficients, the calculations of Deb, Aggarwal & Msezane (1999) were employed for allowed and intercombination lines. Radiative rates for forbidden transitions have also been taken from the work of Deb et al., although the data were not included in the published paper for conciseness. They are available from one of the authors (K.Aggarwal@qub.ac.uk) on request. However, we note that the results are, in general, very similar to those calculated by others, such as Bhatia, Mason & Blancard (1997). A notable exception is the A value for the $3s^2\ ^1S$–$3s3p\ ^3P_2$ transition, where Deb et al. calculate a value of $A = 3.58\ s^{-1}$ compared to the Bhatia et al. result of $A = 0.313\ s^{-1}$. The former is in agreement with the calculation of $A = 3.28\ s^{-1}$ by Bhatia & Kastner (1980) and the unpublished determination of $A = 3.37\ s^{-1}$ by E. Landi in the CHIANTI data base. It is hence clear that the A value listed by Bhatia et al. must be in error. Given that it is wrong by about a factor of 10, this is probably due to a simple typographical error in the exponent for the listed value.

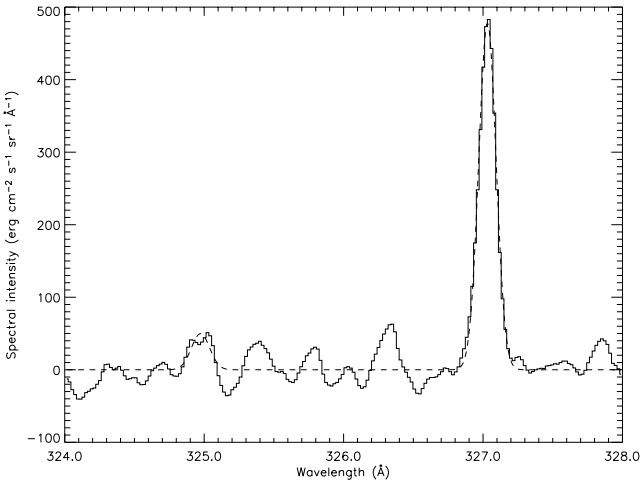

Figure 4. Plot of the SERTS–97 active region spectrum in the 324.0–328.0 Å wavelength range. The profile fit to the Fe XV 324.97- and 327.03-Å features is shown by a dashed line. Also clearly visible in the figure are unidentified emission lines at 325.39, 325.78, 326.32 and 327.85 Å.

For Fe XV, proton impact excitation is only important for transitions among the $3s3p\ ^3P$ levels. In the present analysis we have employed the calculations of Landman & Brown (1979).

Using the atomic data discussed above in conjunction with the Atomic Data and Analysis Structure (ADAS) code (Summers & O'Mullane 2000), relative Fe XV level populations and hence emission-line strengths were calculated for a range of electron temperatures (T_e) and densities (N_e). The following assumptions were made in the calculations: (i) that ionization to and recombination from other ionic levels is slow compared with bound–bound rates; (ii) that photoexcitation and induced de-excitation rates are negligible in comparison with the corresponding collision rates; and (iii) that all transitions are optically thin. Further details of the procedures involved may be found in Summers & O'Mullane.

In Figs 5–9 we plot the theoretical emission-line intensity ratios from R_1 to R_{10}, where the transitions and wavelengths for the lines concerned are listed in Table 1. The ratios are shown as a function of logarithmic electron density at the electron temperature of maximum Fe XV fractional abundance in ionization equilibrium, $T_{max} = 2 \times 10^6$ K, plus ± 0.3 dex about this value, where the fractional abundance has fallen to $N(\text{Fe XV})/N(\text{Fe}) < 0.032$ (Mazzotta et al. 1998). Given errors in the adopted atomic data of typically ± 10 per cent (see the references above), we would expect the theoretical ratios to be accurate to better than ± 20 per cent.

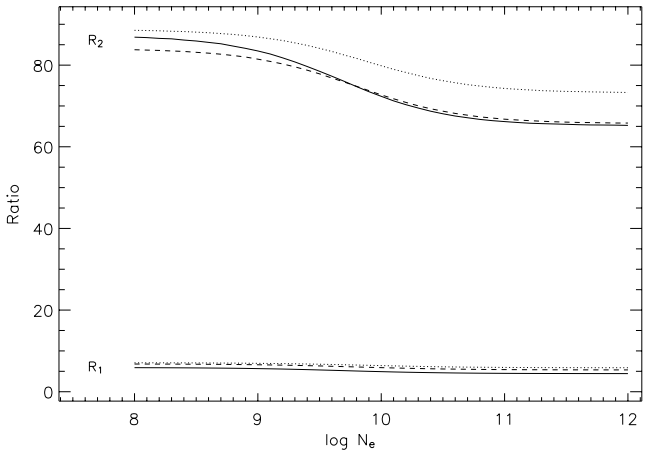

Figure 5. The theoretical Fe XV emission-line ratios $R_1 = I(243.78\ \text{Å})/I(327.03\ \text{Å})$ and $R_2 = I(284.16\ \text{Å})/I(327.03\ \text{Å})$, where I is in energy units, plotted as a function of logarithmic electron density (N_e in cm^{-3}) at electron temperatures of $T_e = 10^6$ K (solid line), $T_e = 2 \times 10^6$ K (dashed line) and $T_e = 4 \times 10^6$ K (dotted line).

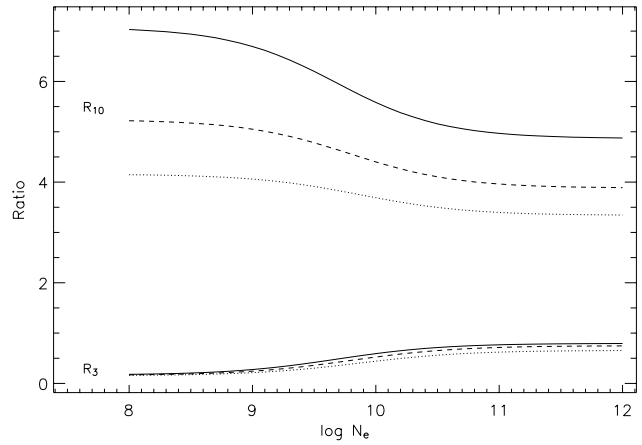

Figure 6. Same as Fig. 5 but for $R_3 = I(292.25\ \text{Å})/I(327.03\ \text{Å})$ and $R_{10} = I(417.25\ \text{Å})/I(327.03\ \text{Å})$.

We note that the ratios R_{11}, R_{12} and R_{13}, also detailed in Table 1, have the same temperature and density dependence as R_3 or R_4, owing to common upper levels, but with

$$R_{11} = 2.72\, R_3,$$

$$R_{12} = 0.697\, R_4,$$

and

$$R_{13} = 0.967\, R_4.$$

Similarly the ratio R_{14} is predicted to have the constant value $R_{14} = 0.592$, owing to common upper levels.

The ratios in Figs 5–9 are given relative to the 327.03-Å transition, as this feature is the cleanest and most reliably detected Fe XV emission line in the SERTS spectra (see Figs 2 and 4). This has been checked by a search of line lists, and also by generating synthetic spectra with CHIANTI, which confirm that no blending species is present which has a line intensity greater than 1 per cent that of the Fe XV 327.03-Å feature. We note that the 284.16-Å line is much stronger and hence better detected than 327.03 Å, but may be subject to opacity effects (Kastner & Bhatia 2001); thus it should not be employed as a reference line. However, theoretical ratios involving any line pair, and for electron temperatures between $T_e = 8 \times 10^5$ and 8×10^6 K, are available from one of the authors (F.Keenan@qub.ac.uk) on request.

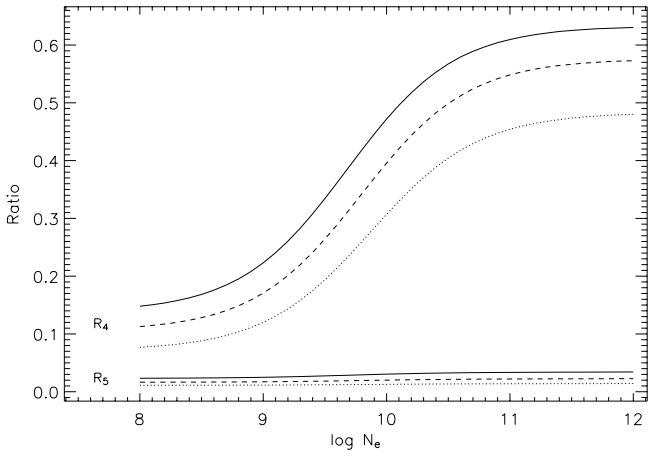

Figure 7. Same as Fig. 5 but for $R_4 = I(302.32\ \text{Å})/I(327.03\ \text{Å})$ and $R_5 = I(317.64\ \text{Å})/I(327.03\ \text{Å})$.

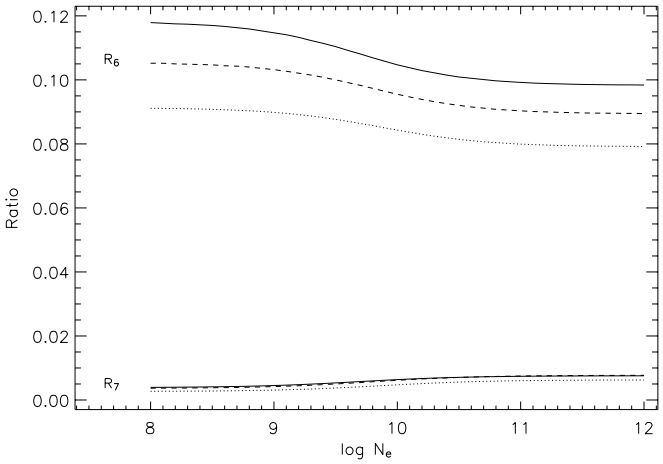

Figure 8. Same as Fig. 5 but for $R_6 = I(324.97\ \text{Å})/I(327.03\ \text{Å})$ and $R_7 = I(330.99\ \text{Å})/I(327.03\ \text{Å})$.

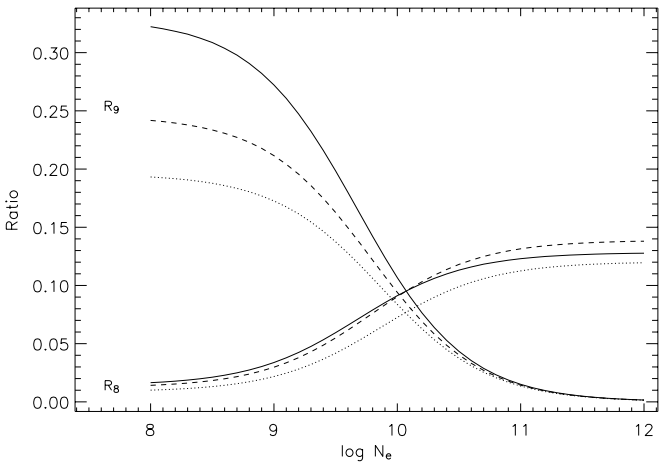

Figure 9. Same as Fig. 5 but for $R_8 = I(372.76\ \text{Å})/I(327.03\ \text{Å})$ and $R_9 = I(393.97\ \text{Å})/I(327.03\ \text{Å})$.

An inspection of Figs 5–9 reveals that several of the ratios are sensitive to variations in the electron density. For example, R_3, R_4 and R_9 vary by factors of 4.2, 4.9 and 16.9, respectively, between $N_e = 10^8$ and 10^{11} cm^{-3}. By contrast, we note that the ratios are relatively insensitive to changes in the adopted electron temperature. For example, increasing T_e from 2×10^6 K to 4×10^6 K (i.e. by a factor of 2) leads to only a 5 per cent decrease in R_3 at $N_e = 10^8$ cm^{-3}, and 6 per cent at $N_e = 10^{11}$ cm^{-3}. In the case of R_4, the variations over the same temperature interval are a decrease of 23 per cent at $N_e = 10^8$ cm^{-3} and 9 per cent at $N_e = 10^{11}$ cm^{-3}. Hence, the ratios should (in principle) provide useful N_e-diagnostics for the Fe XV emitting region of a plasma.

We note that the current line ratios can differ by up to typically 20–30 per cent with other recent calculations, which is within the estimated uncertainty in the theoretical results (see above). For example, at $T_e = 2 \times 10^6$ K and $N_e = 10^8$ cm^{-3}, we calculate $R_3 = 0.17$ and $R_4 = 0.11$, compared to $R_3 = 0.15$ and $R_4 = 0.09$ from the latest version (4.2) of CHIANTI. This version employs radiative data from Griffin et al. (1999), Bhatia et al. (1997) and unpublished calculations by E. Landi, and electron excitation rates from Bhatia et al. However, we note in passing that readers should be aware of a software glitch in version 4.2 of CHIANTI. In the data base, line ratios may be generated using either the CHIANTI_NE or DENS_PLOTTER routines, but the former can provide erroneous results. For example, for the I(417.25 Å)/I(284.16 Å) intensity ratio at $T_e = 2 \times 10^6$ K and $N_e = 10^8$ cm^{-3}, CHIANTI_NE indicates a value of $R = 0.028$, while the true ratio from DENS_PLOTTER is $R = 0.041$. However, the problem has now been fixed (E. Landi, private communication), and the corrected routines will be distributed as part of the next CHIANTI release (version 5).

4 RESULTS AND DISCUSSION

In Tables 2–5 we list the observed Fe XV emission-line ratios measured from the SERTS spectra, along with the associated 1σ errors. Also shown in the tables are the theoretical results from Figs 5–9 at electron densities derived for the SERTS solar features from emission-line ratios in Fe XIII or Fe XIV (Brosius et al. 1996, 2000; Keenan et al. 1996). These species have temperatures of maximum fractional abundance in ionization equilibrium of T_{max}(Fe XIII) $= 1.6 \times 10^6$ K and T_{max}(Fe XIV) $= 2.0 \times 10^6$ K (Mazzotta et al. 1998), close to that for Fe XV. Hence, the Fe XIII and Fe XIV densities should reflect that of the Fe XV emitting plasma in the solar feature. The error bars on the theoretical results are based on the estimated ±20 per cent accuracy of the line ratio calculations (see Section 3).

Table 2. Fe XV emission-line ratios in the SERTS–89 observations.[a]

Ratio	Active region		Subflare	
	Observed[b]	Theoretical[c]	Observed[d]	Theoretical[e]
R_1	6.1 ± 1.2	6.2 ± 1.2	–	6.0 ± 1.2
R_2	83 ± 14	77 ± 15	77 ± 12	74 ± 15
R_3	0.44 ± 0.12	0.39 ± 0.08	0.45 ± 0.12	0.49 ± 0.10
R_8	0.19 ± 0.05	0.062 ± 0.012	0.22 ± 0.06	0.083 ± 0.017
R_9	0.18 ± 0.05	0.15 ± 0.03	0.10 ± 0.03	0.11 ± 0.02
R_{10}	3.9 ± 0.6	4.7 ± 0.9	3.5 ± 0.5	4.5 ± 0.9
R_{11}	2.3 ± 0.3	1.1 ± 0.2	2.4 ± 0.5	1.3 ± 0.3
R_{13}	0.39 ± 0.07	0.28 ± 0.06	0.58 ± 0.11	0.36 ± 0.08
R_{14}	0.77 ± 0.15	0.59 ± 0.12	1.4 ± 0.2	0.59 ± 0.12

Notes. [a]The first-order SERTS–89 bandpass is 235.5–448.7 Å. [b]I(327.03 Å) = 113.3 ± 16.2 erg cm^{-2} s^{-1} sr^{-1}. [c]Determined from Figs 5–7 at $N_e = 10^{9.6}$ cm^{-3}. [d]I(327.03 Å) = 132.0 ± 20.8 erg cm^{-2} s^{-1} sr^{-1}. [e]Determined from Figs 5–7 at $N_e = 10^{9.9}$ cm^{-3}.

Table 3. Fe XV emission-line ratios in the SERTS–91 observations.[a]

Ratio	Active region		Off-limb	
	Observed[b]	Theoretical[c]	Observed[d]	Theoretical[e]
R_2	110 ± 24	77 ± 15	120 ± 33	80 ± 16
R_3	0.69 ± 0.18	0.39 ± 0.08	–	0.30 ± 0.06
R_9	0.24 ± 0.08	0.15 ± 0.03	–	0.19 ± 0.04
R_{10}	3.5 ± 1.2	4.7 ± 0.9	6.4 ± 1.3	4.9 ± 1.0
R_{11}	2.4 ± 0.7	1.1 ± 0.2	2.7 ± 0.7	0.83 ± 0.17
R_{13}	0.47 ± 0.12	0.28 ± 0.06	0.24 ± 0.10	0.21 ± 0.04
R_{14}	0.85 ± 0.20	0.59 ± 0.12	–	0.59± 0.12

Notes. [a]The first-order SERTS–91 bandpass is 231.8–445.3 Å. [b]I(327.03 Å) = 35.4 ± 4.5 erg cm^{-2} s^{-1} sr^{-1}. [c]Determined from Figs 5–9 at $N_e = 10^{9.6}$ cm^{-3}. [d]I(327.03 Å) = 23.6 ± 5.3 erg cm^{-2} s^{-1} sr^{-1}. [e]Determined from Figs 5–7 at $N_e = 10^{9.3}$ cm^{-3}.

Table 4. Fe XV emission-line ratios in the SERTS–93 active region observations.[a]

Ratio	Observed[b]	Theoretical[c]
R_2	110 ± 18	76 ± 15
R_{10}	4.8 ± 0.7	4.6 ± 0.9
R_{11}	2.8 ± 0.5	1.2 ± 0.2
R_{13}	0.33 ± 0.07	0.31 ± 0.06
R_{14}	0.78 ± 0.18	0.59 ± 0.12

Notes. [a]The first-order SERTS–93 bandpass is 231.7–445.4 Å. [b]I(327.03 Å) = 54.7 ± 6.4 erg cm^{-2} s^{-1} sr^{-1}. [c]Determined from Figs 5–9 at $N_e = 10^{9.7}$ cm^{-3}.

Table 5. Fe XV emission-line ratios in the SERTS–97 active region observations.[a]

Ratio	Observed[b]	Theoretical[c]
R_4	0.48 ± 0.15	0.29 ± 0.06
R_5	0.054 ± 0.041	0.019 ± 0.004
R_6	0.10 ± 0.05	0.10 ± 0.02
R_7	0.083 ± 0.050	0.0052 ± 0.0010
R_{11}	1.4 ± 0.3	1.1 ± 0.2
R_{12}	0.58 ± 0.16	0.20 ± 0.04
R_{13}	0.31 ± 0.08	0.28 ± 0.06
R_{14}	0.66 ± 0.17	0.59 ± 0.12

Notes. [a]The first-order SERTS–97 bandpass is 299.0–353.5 Å. [b]I(327.03 Å) = 74.6 ± 12.2 erg cm^{-2} s^{-1} sr^{-1}. [c]Determined from Figs 5–9 at $N_e = 10^{9.6}$ cm^{-3}.

An inspection of Tables 2–5 reveals good agreement between theory and observation for the R_1, R_2, R_3, R_9, R_{10} and R_{13} ratios. This indicates that the 243.78-, 292.25-, 321.78-, 327.03-, 393.97- and 417.25-Å emission lines of Fe XV are well observed in the SERTS spectra, are free from significant blends, and hence may be employed as reliable diagnostics. Our results also imply that the 284.16-Å line is optically thin, at least in the solar features under consideration. In addition, we confirm the identifications by Young et al. (1998) and Brickhouse et al. (1995) of the 292.25- and 393.97-Å features as the 3s3p ^{3}P$_1$–3p^2 ^{3}P$_2$ and 3s^2 ^{1}S–3s3p ^{3}P$_2$ transitions, respectively, of Fe XV.

The observed R_4, R_5 and R_{12} ratios are all larger than the theoretical values, suggesting that the 302.32-, 317.64- and 307.76-Å lines

are blended, with the species responsible contributing around 40, 65 and 65 per cent to the total measured 302.32-, 317.64- and 307.76-Å fluxes, respectively. The blending line for the 302.32-Å feature is clearly the $3s^2 3p^3\ ^4S$–$3s3p^4\ ^4P_{3/2}$ transition of Ni XIV. Although the line is identified as being due to Fe XV in Brosius et al. (2000), it is listed as Ni XIV by Thomas & Neupert (1994) in the original SERTS catalogue. Our analysis indicates that both sets of authors are partially correct, with the 302.32-Å line intensity being attributable to Fe XV and Ni XIV in approximately equal measures.

For the 307.76- and 317.64-Å lines, synthetic spectra generated with CHIANTI indicate that the blending species are Si VIII $2s^2 2p^3\ ^2P_{1/2}$–$2s2p^4\ ^2D_{3/2}$ and Na VI $2s^2 2p^2\ ^1D$–$2s2p^3\ ^1P$, respectively. The CHIANTI calculations predict that the Si VIII and Na VI transitions will contribute approximately 50 and 70 per cent to the 307.76- and 317.64-Å line intensities, respectively, in good agreement with our observations.

The measured R_7 ratio is more than a factor of 10 larger than predicted by theory, indicating that Fe XV is at best a minor contributor to the 330.99-Å emission feature in solar spectra. Synthetic spectra from CHIANTI indicate that there is no feature in this wavelength region with a predicted intensity greater than 10 per cent that of the Fe XV line. However, the strong $2s^2 2p^5\ ^2P_{3/2}$–$2s2p^6\ ^2S$ resonance line of Ar X lies at 165.53 Å, and it possible that this is a second-order feature in the SERTS spectrum, appearing in first order at around 331 Å. Support for this comes from the fact that the $2s^2 2p^5\ ^2P_{1/2}$–$2s2p^6\ ^2S$ line of Ar X at 170.643 Å is predicted to lie at a wavelength of 341.286 Å in first order, with an intensity of 45 per cent that of the 165.53-Å transition. In the SERTS–97 active region spectrum, there is an unidentified feature at 341.285 Å, with an intensity of approximately 65 per cent that of 330.99 Å. We therefore believe that the observed 330.99- and 341.285-Å features are indeed the second-order Ar X lines.

Keenan et al. (1993) have suggested that a line observed at 324.97 Å in solar flare spectra obtained with the S082A instrument on *Skylab* is the $3s3p\ ^1P$–$3p^2\ ^1S$ transition of Fe XV. Young et al. (1998) have cast doubt on this identification, on the basis that the intensity ratio $R_6 = I(324.97\ \text{Å})/I(327.03\ \text{Å})$ is predicted to be density-insensitive and to have a value of $R_6 = 0.025$, while the average measured ratio from the *Skylab* spectra is $R_6 = 0.09$. Brosius et al. (2000) similarly note that the measured R_6 ratio in the SERTS–97 spectrum ($R_6 = 0.10 \pm 0.05$) is much larger than predicted by CHIANTI, indicating that the 324.97-Å feature is very badly blended with emission from other ion(s), or that the atomic physics need to be revised. However, as may be seen from Fig. 8, we calculate a theoretical ratio of $R_6 = 0.10$, as does the latest version of CHIANTI. These are in excellent agreement with both the SERTS–97 measurement (Table 5) and the *Skylab* data of Keenan et al. Hence, our new theoretical results do in fact indicate that the 324.97-Å line is due to Fe XV.

Except for the SERTS–97 results, observed values of R_{11} are typically about a factor of 2.3 larger than predicted, confirming that the 304.87-Å line is often significantly blended with Mn XIV, as originally suggested by Thomas & Neupert (1994). However, these authors also noted that the 312.55-Å line is blended with a Co XVII transition. By contrast, our results for R_{14} indicate good agreement between theory and observation for the solar active region data sets, implying that Co XVII makes a minor contribution to the blend, averaging around 22 per cent. Only in the subflare, where the measured R_{14} ratio is a factor of 2.4 larger than theory, does Co XVII make a major contribution. This is not surprising, as Co XVII is formed at a higher temperature than Fe XV, $T_{\max}(\text{Co XVII}) = 3.2 \times 10^6$ K (Mazzotta et al. 1998), and hence would be expected to be relatively stronger in flares compared to active regions.

Young et al. (1998) have suggested that the 372.76-Å line in the SERTS–89 active region spectrum has been misidentified as the $3s3d\ ^3D_3$–$3p3d\ ^3F_4$ transition of Fe XV by Thomas & Neupert (1994), as the theoretical intensity is much lower than that observed. However, our results for the R_8 ratio indicate that Fe XV does in fact make a significant contribution (about 35 per cent) to the 372.76-Å line intensities in both the SERTS–89 active region and subflare. Unfortunately, an inspection of line lists and synthetic spectra from CHIANTI does not indicate any likely blending species in first or second order, and hence more work is required to identify the blend.

Finally, Flower & Jordan (1971) first noted that there is a discrepancy between theory and observation for the Fe XV intercombination to allowed line intensity ratio, $R = I(417.25\ \text{Å})/I(284.16\ \text{Å})$, with experimental values being much larger than the theoretical ones (see also Feldman et al. 1992). For example, Young et al. (1998) measured the ratio to be $R_{\text{obs}} = 0.045 \pm 0.007$ in the SERTS–89 active region spectrum, compared to a theoretical value of $R_{\text{theory}} = 0.031$ from version 1 of CHIANTI (Dere et al. 1997), which employed the radiative and electron collisional data of Bhatia et al. (1997). By contrast, our averaged observed ratio in the SERTS data sets is $R_{\text{obs}} = 0.045 \pm 0.010$, while we calculate $R_{\text{theory}} = 0.061$, and the latest version (4.2) of CHIANTI indicates $R_{\text{theory}} = 0.040$. Although this may appear to imply that agreement between theory and experiment is better for the CHIANTI results, we note that any comparison of R ratio calculations with SERTS observations must be treated with caution. This is due to the fact that the SERTS instrument calibration is uncertain for wavelengths longward of 400 Å, as noted by Young et al. (1998), and was determined using the line ratio technique prior to the SERTS–97 mission. As the 284.16t and 417.25tÅ emission lines of Fe XV are very strong and well detected (providing instrument response values with very small error bars), and also so well separated in wavelength, their ratio played a significant role for each SERTS flight in setting an overall shape for the relative calibration curve beyond 400 Å. Consequently, the final calibration curve was one which forced all measured R ratios to be as close as possible to the then available predicted value (consistent with all other ratios from similar wavelengths). The theoretical R ratio employed for the SERTS–89 data was $R_{\text{theory}} = 0.031$, and hence it is not surprising that the observed values of R are close to this. By contrast, if we adopt our theoretical value of $R_{\text{theory}} = 0.061$ for the calibration, this leads to $R_{\text{obs}} = 0.056$, improving the agreement with the present calculation. Clearly, independent (well-calibrated) measurements of the R ratio are required to resolve this problem, and hence determine if the present calculations or those from CHIANTI (or indeed neither) are to be preferred. We note in passing that Dere (1982) finds an average $R_{\text{obs}} = 0.063$ for two active regions observed by *Skylab*, which would appear to be in excellent agreement with the present theory. However, the individual *Skylab* measurements ($R = 0.040$ and 0.086) differ significantly, and hence cannot be treated with confidence.

ACKNOWLEDGMENTS

KMA and VS acknowledge financial support from the EPSRC, RSIR and DSB from the UK Particle Physics and Astronomy Research Council (PPARC), while ROM is grateful to the Department of Education and Learning (Northern Ireland) and to NASA's Goddard Space Flight Center for the award of a studentship. The SERTS rocket programme is supported by RTOP grants from the Solar Physics Office of NASA's Space Physics Division. JWB acknowledges additional NASA support under grant NAG5–13321.

FPK is grateful to AWE Aldermaston for the award of a William Penney Fellowship. The authors thank Peter van Hoof for the use of his Atomic Line List. CHIANTI is a collaborative project involving the Naval Research Laboratory (USA), Rutherford Appleton Laboratory (UK), and the Universities of Florence (Italy) and Cambridge (UK).

REFERENCES

Aggarwal K. M., Keenan F. P., Msezane A. Z., 2003, A&A, 410, 349
Bely O., Blaha M., 1968, Solar Phys., 3, 563
Bhatia A. K., Kastner S. O., 1980, Solar Phys., 65, 181
Bhatia A. K., Mason H. E., Blancard C., 1997, At. Data Nucl. Data Tables, 66, 83
Brickhouse N. S., Raymond J. C., Smith B. W., 1995, ApJS, 97, 551
Brosius J. W., Davila J. M., Thomas R. J., Monsignori-Fossi B. C., 1996, ApJS, 106, 143
Brosius J. W., Davila J. M., Thomas R. J., 1998, ApJS, 119, 255
Brosius J. W., Thomas R. J., Davila J. M., Landi E., 2000, ApJ, 543, 1016
Churilov S. S., Kononov E. Y., Ryabtsev A. N., Zayikin Y. F., 1985, Phys. Scripta, 32, 501
Churilov S. S., Levashov V. E., Wyart J. F., 1989, Phys. Scripta, 40, 625
Deb N. C., Aggarwal K. M., Msezane A. Z., 1999, ApJS, 121, 265
Dere K. P., 1978, ApJ, 221, 1062
Dere K. P. 1982, Solar Phys., 77, 77
Dere K. P., Landi E., Mason H. E., Monsignori-Fossi B. C., Young P. R., 1997, A&AS, 125, 149
Feldman U., Laming J. M., Mandelbaum P., Goldstein W. H., Osterheld A., 1992, ApJ, 398, 692
Flower D. R., Jordan C., 1971, A&A, 14, 473
Griffin D. C., Badnell N. R., Pindzola M. S., Shaw J. A., 1999, J. Phys. B, 32, 2139
Howarth I. D., Murray J., Mills D., 1994, Starlink User Note No. 50.15
Kastner S. O., Bhatia A. K., 2001, ApJ, 553, 421
Keenan F. P., Dufton P. L., Conlon E. S., Foster V. J., Kingston A. E., Widing K. G., 1993, ApJ, 405, 798
Keenan F. P., Thomas R. J., Neupert W. M., Foster V. J., Brown P. J. F., Tayal S. S., 1996, MNRAS, 278, 773
Keenan F. P. et al., 2000, MNRAS, 315, 450
Landman D. A., Brown T., 1979, ApJ, 232, 636
Litzen U., Redfors A., 1987, Phys. Scripta, 36, 895
Mazzotta P., Mazzitelli G., Colafrancesco S., Vittorio N., 1998, A&AS, 133, 403
Neupert W. M., Epstein G. L., Thomas R. J., Thompson W. T., 1992, Solar Phys., 137, 87
Sugar J., Corliss C., 1985, J. Phys. Chem. Ref. Data Suppl., 2, 484
Summers H. P., O'Mullane M. G., 2000, AIP Conf. Proc. Vol. 543, Atomic and Molecular Data and their Applications. American Institute of Physics, New York, p. 304
Thomas R. J., Neupert W. M., 1994, ApJS, 91, 461
Young P. R., Landi E., Thomas R. J., 1998, A&A, 329, 291
Young P. R., Del Zanna G., Landi E., Dere K. P., Mason H. E., Landini M., 2003, ApJS, 144, 135

This paper has been typeset from a TEX/LATEX file prepared by the author.